

Title	Study on Electron Beam Welding of Dissimilar Materials for Nuclear Plant (Report I) : Effect of Welding Conditions on Weld Defects(Welding Physics, Process & Instrument)
Author(s)	Arata, Yoshiaki; Shimizu, Shigeki; Murakami, Takashi
Citation	Transactions of JWRI. 1983, 12(2), p. 183-192
Version Type	VoR
URL	<a href="https://doi.org/10.18910/11093">https://doi.org/10.18910/11093</a>
rights	
Note	

***Osaka University Knowledge Archive : OUKA***

<https://ir.library.osaka-u.ac.jp/>

Osaka University

# Study on Electron Beam Welding of Dissimilar Materials for Nuclear Plant (Report I)<sup>†</sup>

— Effect of Welding Conditions on Weld Defects —

Yoshiaki ARATA\*, Shigeki SHIMIZU\*\* and Takashi MURAKAMI\*\*

## Abstract

In this paper, the weldability of some combinations of dissimilar materials for nuclear plant is investigated using electron beam welding, and the region of adequate welding condition is obtained for each combination of dissimilar materials. The results obtained are summarized as follows:

- (1) Kinds of weld defects are R-porosity and micro crack (nail-head crack and horizontal and vertical crack).
- (2) R-porosity occurs in all the combination with no relation to the materials, and it generates within the specific range of  $ab$  value.
- (3) Most of nail-head crack occurs in the combination with Inconel 617, and runs almost normal to bond at nail head of Inconel 617 side. This crack occurs almost without respect to welding condition.
- (4) The solidification crack of horizontal and vertical type is observed mostly in the combination with Incoloy 800H. This crack generates at lower or higher than the specific  $ab$  value.
- (5) The region of adequate welding condition where non-defect occurs is found to exist in the thickness less than about 15 mm except for the combination with Inconel 617.

**KEY WORDS:** (Electron Beam Welding) (Superalloy) (Dissimilar Welded Joint) (Weld Defect) (Weldability)

## 1. Introduction

In component for high temperature gas cooled reactor (HTR), design temperature widely ranges from 400 to 1000°C, and so component materials are different from temperature of the place where they are used.

As shown in **Figure 1**, Ni-base superalloys of Hastelloy type and Inconel type are used in high temperature range. As it becomes lower temperature, Fe-base superalloys of Incoloy type, austenitic stainless steel and ferritic low-alloy steel are used.

At the boundaries between these temperature ranges, it is essential to use the welded joints of dissimilar materials, resulting in the design requirement to evaluate high temperature strength of welded joints and to establish the adequate welding procedure for the combinations of dissimilar materials.

In this paper, the effect of welding conditions on the weld defects in the electron beam welding, which is said to be effective for welding the dissimilar materials, is examined for the most probable combinations of dissimilar materials. Besides, the region of adequate welding conditions is obtained for each combination of dissimilar materials.

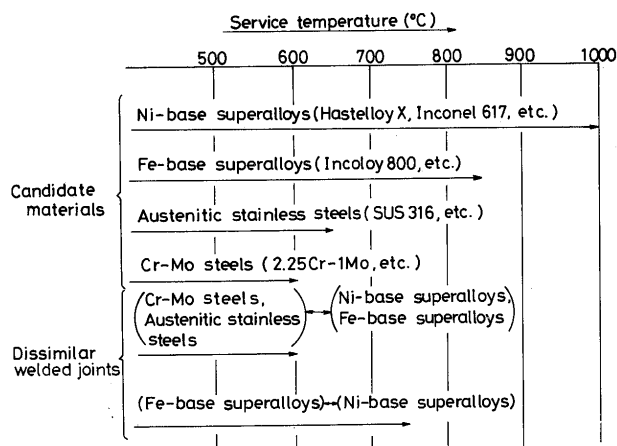


Fig. 1 Materials and combinations of dissimilar materials used for high temperature gas cooled reactor

## 2. Material Used

The chemical composition of the materials used in this experiment is listed in **Table 1**. In this experiment, Hastelloy X, Inconel 625 and Inconel 617 are selected as Ni-base superalloys, Incoloy 800H as Fe-base superalloy, SUS316 and SUS304 as austenitic stainless steels, and

<sup>†</sup> Received on October 31, 1983

\* Professor

\*\* Kawasaki Heavy Industries, Ltd., Japan

Table 1 Chemical compositions of materials used

Material	C	Si	Mn	P	S	Ni	Cr	Mo	Cu	Al	Ti	Co	Ni+Ta	W	Fe
Hastelloy X	0.08	0.46	0.70	0.015	<0.005	Bal.	21.18	8.82	—	—	—	0.99	—	0.48	18.03
Inconel 625	0.05	0.33	0.33	0.004	<0.005	Bal.	22.26	9.11	—	0.23	0.14	0.10	3.29	—	2.78
Inconel 617	0.09	0.19	0.03	—	0.004	Bal.	21.09	9.04	—	1.05	—	12.52	—	—	1.42
Incoloy 800H	0.05	0.29	0.80	0.014	0.009	33.93	20.09	—	0.27	0.49	0.45	—	—	—	Bal.
SUS 316	0.05	0.88	1.70	0.031	0.007	11.63	17.89	2.28	—	—	—	—	—	—	Bal.
SUS 304	0.06	0.51	1.02	0.036	0.003	8.66	18.12	—	—	—	—	—	—	—	Bal.
2.25Cr - 1Mo	0.07	0.27	0.55	0.011	0.003	—	2.20	0.98	—	—	—	—	—	—	Bal.

2.25Cr-1Mo steel as ferritic low-alloy steel.

### 3. Welding and Experimental Method

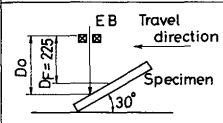
#### 3.1 Welding Equipment

The electron beam welding equipment used in this experiment is that of full vacuum type and of high voltage type, whose maximum power is 6 KW (150KV - 40mA).

#### 3.2 Welding Method

Out of each material shown in Table 1, welding test specimens of  $30^t \times 10^w \times 280^l$  are made. The specific combination of the dissimilar materials is selected to build the gap-free square butt welded joints. Several pairs of the joints are restrained in parallel with jig, and the slope welding, whose slope angle ( $\theta_s$ ) is 30 degrees, as shown in Table 2, is conducted one by one in upward direction to continuously change  $a_b$  value. In this Table welding conditions used in this experiment are also shown. Parameter  $V_b$ ,  $I_b$  and  $v_b$  are changed in the welding. Parameter  $D_o$  is changed continuously with the slope welding.

Table 2 Electron beam welding condition

Slope welding method	$V_b$ (kV)	$I_b$ (mA)	$v_b$ (cm/min)	$D_F$ (mm)	$D_o$ (mm)	$P_{ch}$ (Torr)
	100	20	60	225	155	$5 \times 10^{-4}$
	125	30	100			
	150	40	160			

#### 3.3 Combinations of Dissimilar Materials

In this experiment, the electron beam welding, as described in the previous section (i.e. section 3.2), is conducted to each combination of dissimilar materials which is shown in Table 3. Also shown in the Table are the welding parameters such as  $V_b$ ,  $I_b$ ,  $v_b$ ,  $W_b$  and heat input  $q$ , which are used in the welding.

Table 3 Combinations of dissimilar materials

Combination of materials *1	Welding *2 condition	Combination of materials *1	Welding *2 conditions
HX / 617	1,2,3	617 / Cr-Mo	1,2,3
HX / 800	1,2,3,4,5,6,7,8,9	625 / 800	1,2,3,6
HX / 316	1,2,3,4,5,6,7,8,9	625 / 316	1,2,3,4,5,6
HX / 304	1,2,3,4,5,6,7,8,9	625 / 304	1,2,3,4,5,6
HX / Cr-Mo	1,2,3,4,5,6	625 / Cr-Mo	1,2,3
617 / 800	1,2,3,4,5,6	800 / 316	1,2,3,4,5,6
617 / 316	1,2,3,4,5,6	800 / 304	1,2,3,4,5,6
617 / 304	1,2,3,4,5,6	800 / Cr-Mo	1,2,3,4,5,6

\*1 HX : Hastelloy X, 617 : Inconel 617, 800 : Incoloy 800H  
316 : SUS316, 304 : SUS304, Cr-Mo : 2.25Cr-1Mo,  
625 : Inconel 625

\*2

Mark	$V_b$ (kV)	$I_b$ (mA)	$v_b$ (cm/min)	$W_b$ (kw)	$q$ (Joule/cm)
1	150	40	100	6.0	3,600
2	150	40	160	6.0	2,250
3	150	40	60	6.0	6,000
4	150	30	60	4.5	4,500
5	100	30	60	3.0	3,000
6	100	30	160	3.0	1,125
7	100	20	100	2.0	1,200
8	125	40	100	5.0	3,000
9	125	30	100	3.75	2,250

#### 3.4 Experimental Method

For each welded joint, X-ray inspection from side is performed to examine defects of weld zone. Mainly concerned are a porosity at penetration edge. After finishing X-ray inspection, test specimens of cross section which has the slope angle of 30 degrees, are sampled at 20 mm interval from each welded joint. The cross section of the specimen is polished and etched, and then macrostructure observation and measurement of penetration depth and of bead width are performed on this cross section. Microstructure and weld defects, such as porosity, micro crack

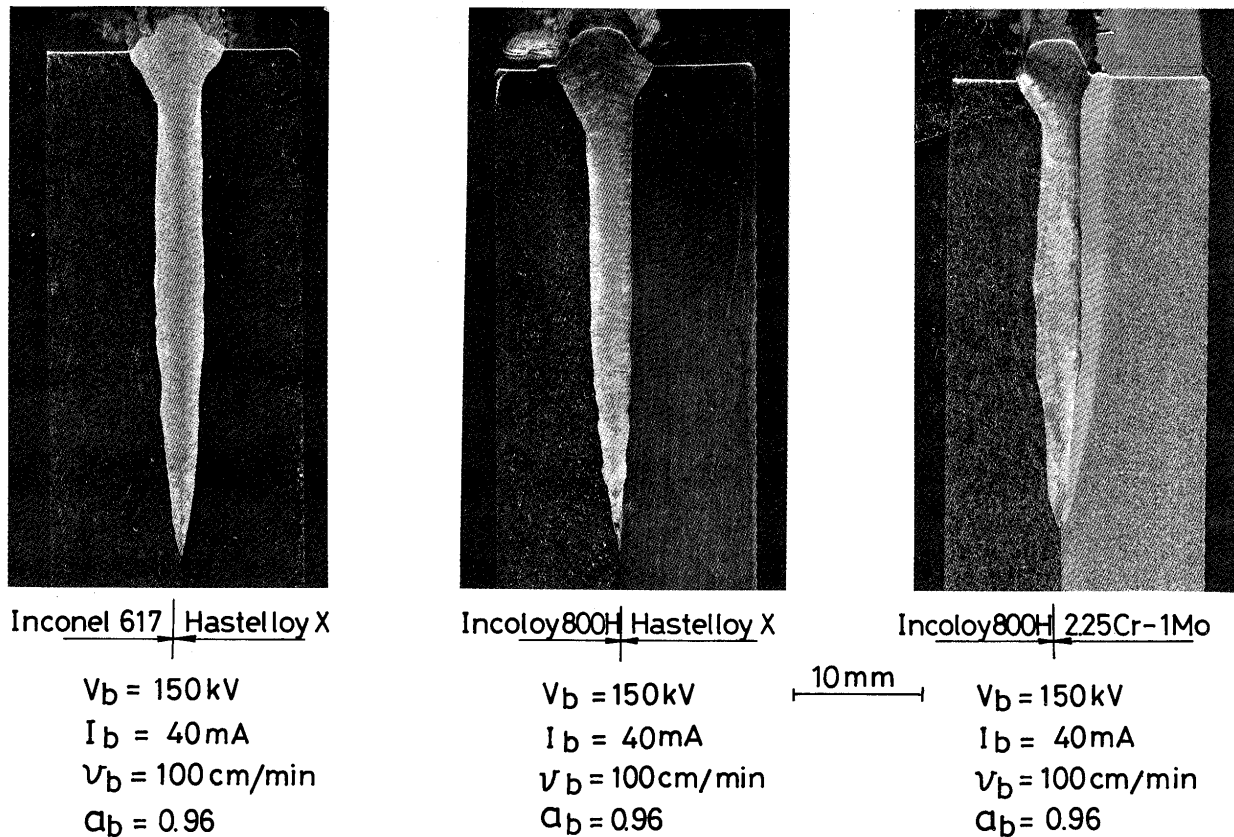


Fig. 2 Macrostructure of welded joints

and others, of weld zone are also examined. Picking up the typical micro crack, the changes in compositions at around the zone are investigated with line analysis by electron probe microanalyzer (EPMA).

#### 4. Experimental Results and Discussions

##### 4.1 Appearance of Cross Section at Weld Zone

An example of cross section macrostructure at electron beam welded joint of dissimilar materials is shown in Figure 2. At each welded joint, welding has been done such a manner as to locate the center of electron beam at the center of square butt welded joint (i.e. at the boundary of both materials). There has been observed almost the same penetration status even for such combination of dissimilar materials as between austenitic materials (i.e. Ni and Fe-base superalloys and austenitic stainless steel), and between austenitic materials and ferritic low-alloy steel (2.25Cr-1Mo). They show the almost symmetrical penetration configuration, centered around the original square butt welded joint. Provided that welding conditions (i.e.  $V_b$ ,  $I_b$ ,  $v_b$  and  $\alpha_b$  values) are the same, such configuration of bead cross section as penetration depth  $h_p$  and bead width  $d_B$  is same even for different combi-

nations of materials.

##### 4.2 Weld Defects

As results of X-ray inspection of weld zone and microstructure observation of cross section, several defects are found at weld zone depending on the combination of dissimilar welded joints and on the difference in the welding conditions.

In Figure 3, the types and major locations of the weld defects, observed on the cross section of dissimilar welded

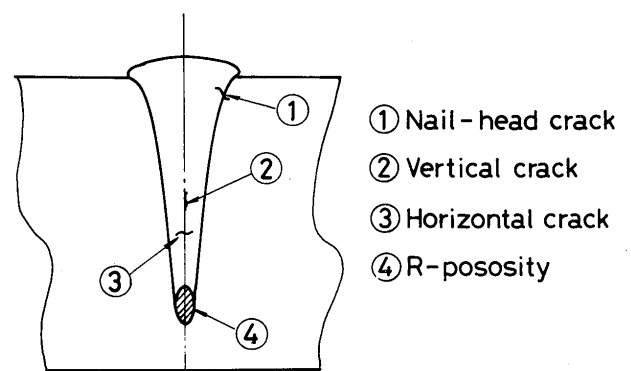


Fig. 3 Schematic configuration of weld defects occurred in dissimilar welded joint

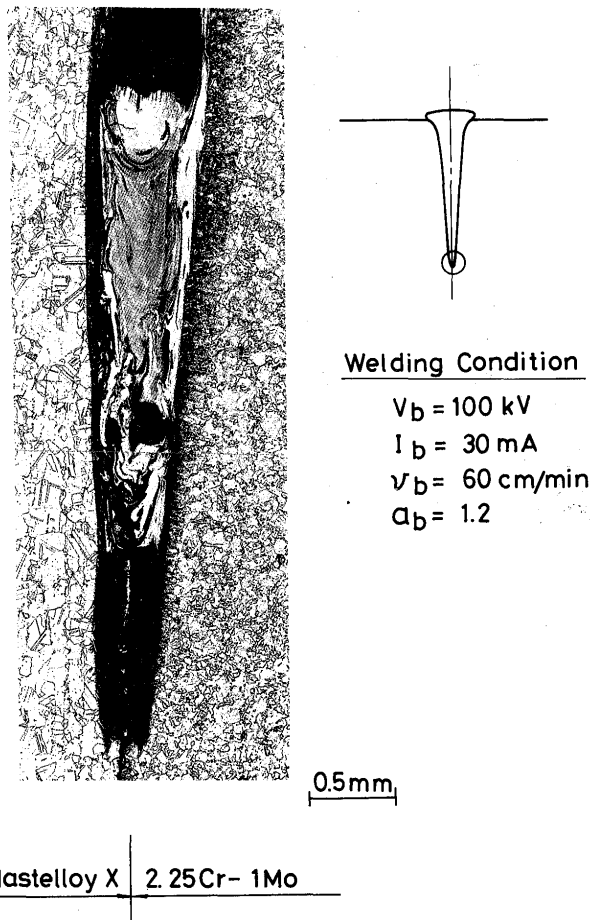


Fig. 4 Appearance of R-porosity

joints, are illustrated. Types of weld defects are root porosity (R-porosity) and micro crack (nail-head crack, horizontal and vertical crack). Explanation for each type and the relation with welding conditions are described in the followings.

#### (1) Porosity

An example of porosity is shown in **Figure 4**. Almost all the porosity observed is R-Porosity<sup>1)</sup>, which is observed at tip of penetration (i.e. root of weld), and has void of 3 to 4 mm deep at the worst. **Table 4** shows the percentage index of number of R-porosity divided by total number of test specimens. Though the welding conditions, such as  $V_b$ ,  $I_b$ ,  $v_b$  and  $a_b$  values, are not considered in this result, the effect of combinations of materials on the R-porosity percentage is not clear. The existence of R-porosity is depended to  $a_b$  value and penetration depth, and this is described in section 4.3.

#### (2) Micro crack

##### (i) Nail-head crack

An example of nail-head crack is shown in **Figure 5**. As

Table 4 Percentage of weld defects occurred in dissimilar welded joints (%)

Combinations	R-porosity	Micro crack		
		Nail-head	Horizontal	Vertical
HX / 617	25.6	59.0(617)* <sup>1</sup>	12.8	2.6
HX / 800	14.5	0	6.0	0.9
HX / 316	8.5	0.9(HX)	3.4	1.7
HX / 304	10.3	0.9(304)	4.3	0
HX/Cr-Mo	7.7	2.6(HX)	0	0
617 / 800	16.7	48.7(617)	5.1	0
617 / 316	9.0	57.7(617)	0	1.3
617 / 304	19.2	65.4(617)	7.7	1.3
617/Cr-Mo	15.4	79.5(617)	0	0
625 / 800	5.8	0	0	0
625 / 316	20.5	0	0	0
625 / 304	14.9	0	0	0
625 /Cr-Mo	10.3	0	7.7	2.6
800 / 316	15.4	0	23.1	1.3
800 / 304	7.7	1.3(800)	26.9	3.8
800 /Cr-Mo	6.4	3.8(800)	19.2	10.3

\*1 Material on which nail-head crack occurred.

shown in **Fig. 3**, this crack generates at the nail head on the cross section of weld zone, and at nearly normal angle to bond on the weld metal and on the heat affected zone. The crack runs the grain boundary on heat affected zone and the dendrite boundary on weld metal.

The percentage index of number of nail-head crack divided by total number of test specimens was shown in **Table 4** for each combination of dissimilar materials. As can be seen from **Table 4**, generation of the nail-head crack is predominantly high at bond of Inconel 617 side. As for combination of Inconel 617 with other dissimilar materials, the crack percentage is almost 50% or more without respect to combination with any other materials. In other words, crack will exist one per two test specimens of cross section. Though it seldom exist at bond of other materials, a few cracks are observed at bond of Hastelloy X, Incoloy 800H and SUS304.

Nail-head crack is the micro crack of 20 to 300  $\mu\text{m}$  long, and is considered as same kind of the nail-head crack as observed at electron beam weld zone of superalloys for nuclear plants<sup>2)</sup>. For example, sensitivity of nail-head crack generation at the electron beam weld zone for the same materials is predominantly high for Inconel 617, and is negligible for Inconel 625 and SUS316<sup>2)</sup>.

##### (ii) Horizontal and Vertical Crack

A type of horizontal crack observed in weld metal is shown in **Figure 6**. As shown in **Fig. 3**, this crack runs nearly horizontally along the dendrite boundary on the bead section, and is 20 to 400  $\mu\text{m}$  long. A type of vertical

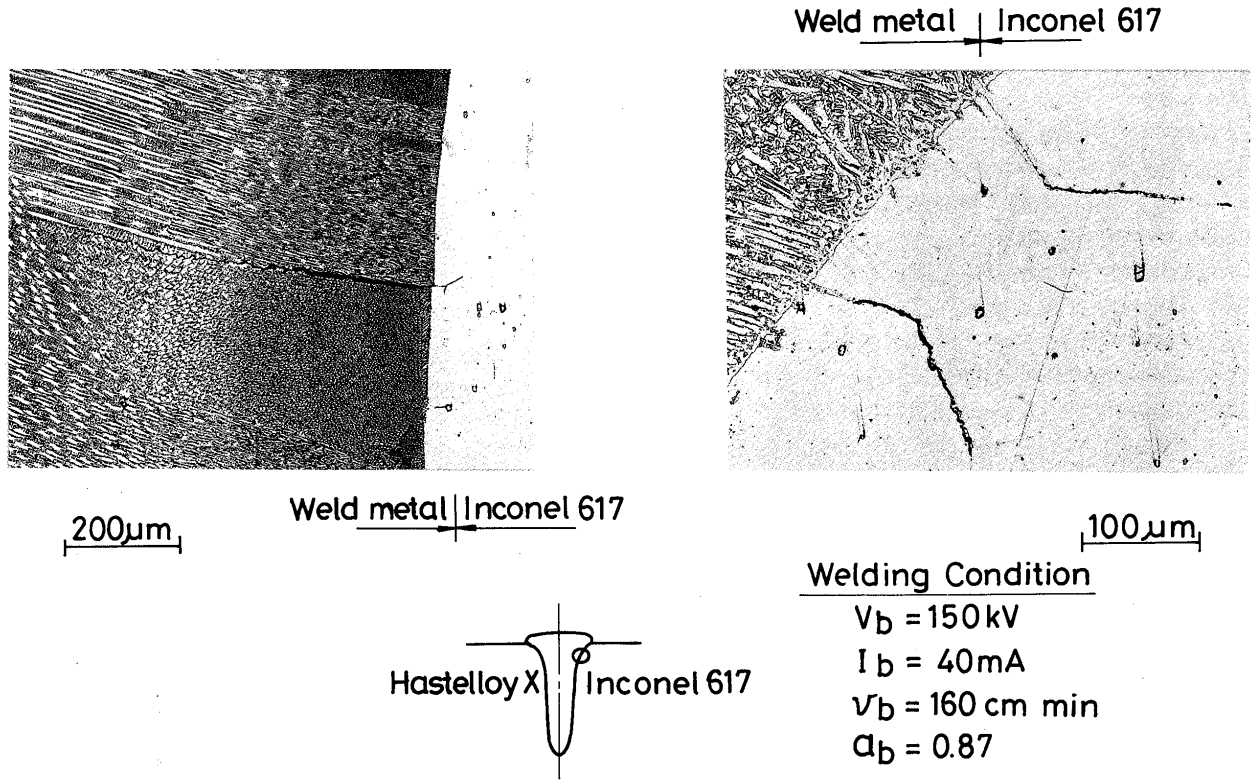


Fig. 5 Appearance of nail-head crack

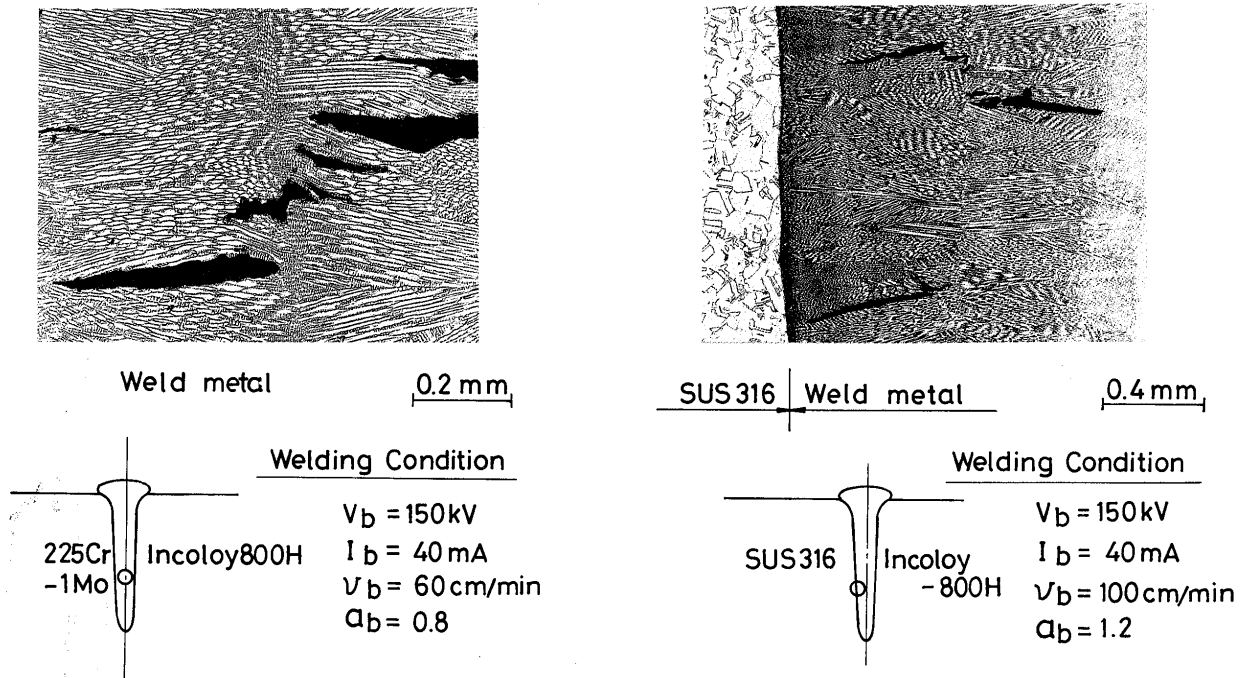


Fig. 6 Appearance of horizontal crack

crack as observed on weld metal is shown in **Figure 7**. As shown in Fig. 3, this crack runs vertically along the interface of column structure at the center of bead (i.e. at around the original center of square butt welded joint) on

the bead section, and is 20 to 40 μm long.

The types of these micro cracks are different, but they are considered to belong to the solidification crack of weld metal. **Figure 8** is the result of EPMA line analysis,

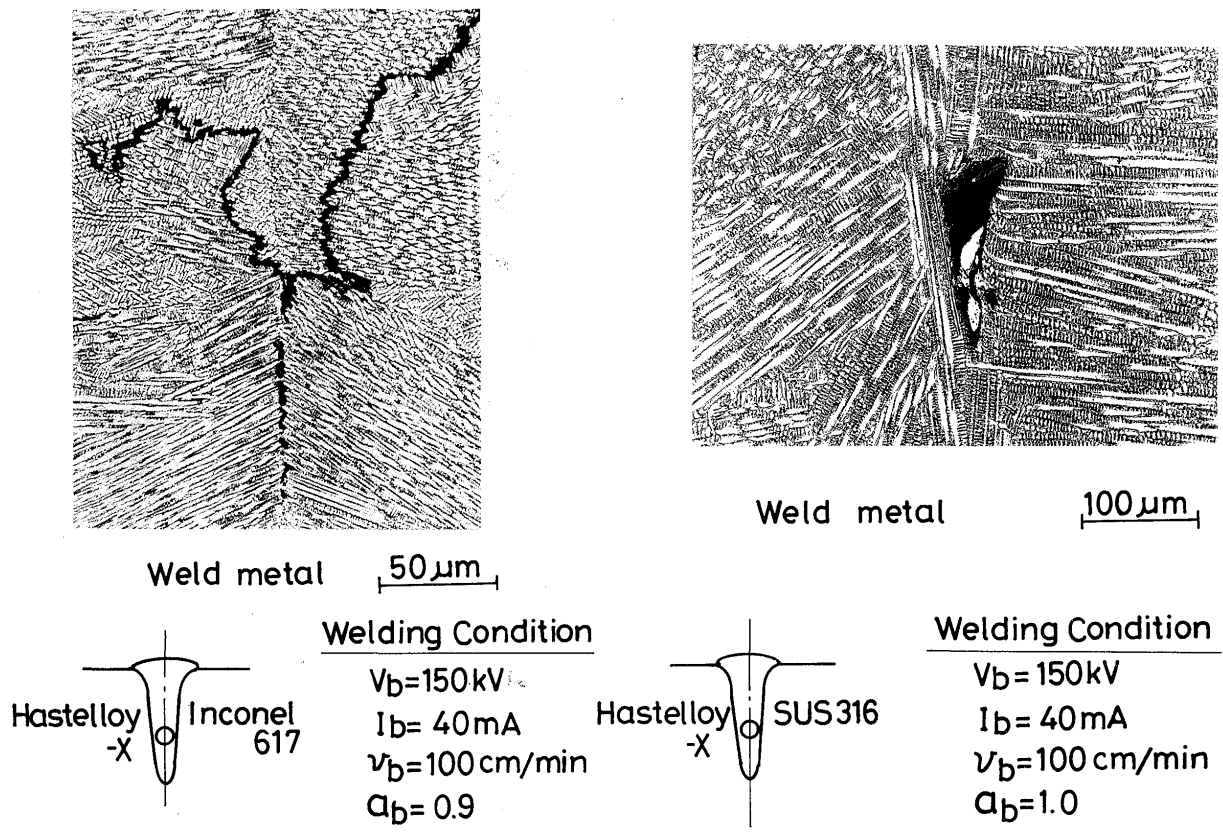


Fig. 7 Appearance of vertical crack

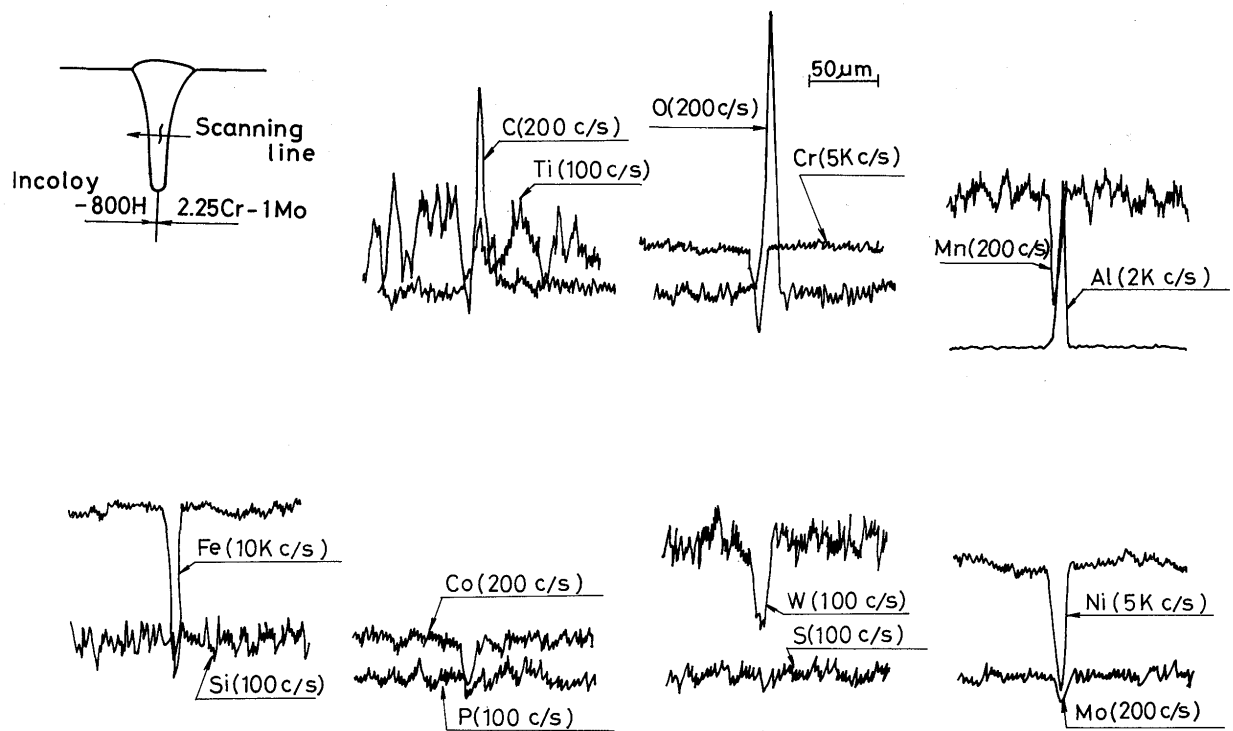


Fig. 8 Profile of elements at micro crack analyzed by EPMA

which is performed normal to the vertical crack generated in combination of Incoloy 800H and 2.25Cr-1Mo steel. In crack, C, Al and O are observed to be rich, whereas Fe, Ni, Cr and W are depleted. The similar tendency is observed in the horizontal and vertical crack of another combination of dissimilar materials. The analysis results of micro crack generated on electron beam weld zone of dissimilar superalloys (Inconel 718/Inconel 713), performed in another organization show the similar tendency<sup>3)</sup>.

For each combination of dissimilar materials, the percentage index of number of horizontal and vertical cracks divided by total number of test specimens was shown in Table 4. As can be seen from Table 4, combinations with Incoloy 800H have generally the high probability of horizontal and vertical crack out of the combination of dissimilar materials. On the other hand, only the combination with 2.25Cr-1Mo steel out of that with Inconel 625 shows the crack, and neither horizontal nor vertical crack is generated on other combinations. It is reported that the weld zone of Inconel 625 by electron beam welding has superior resistance of crack sensitivity than other superalloys, and it is said that this is due to Nb in the compositions<sup>4)</sup>.

Figure 9 shows the relation between welding heat input  $q (= 60 \times V_b \times I_b / v_b)$  and horizontal crack percentage for combinations with Incoloy 800H. It is generally said that the more welding heat input, the more solidification crack, but this relation is not clear for other combinations though Incoloy 800H/2.25Cr-1Mo steel combination which has similar relation as above in this experiment.

Relation between horizontal crack percentage and beam power  $W_b (= V_b \times I_b)$  is shown in Figure 10. The dissimilar welded joints of Incoloy 800H with 2.25Cr-1Mo steel, SUS304 and SUS316 show higher crack sensitivity as increase in  $W_b$ , whereas these of Incoloy 800H

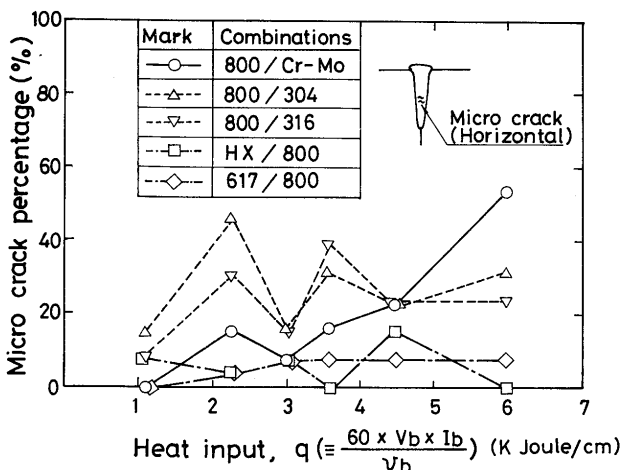


Fig. 9 Effect of heat input on micro crack percentage

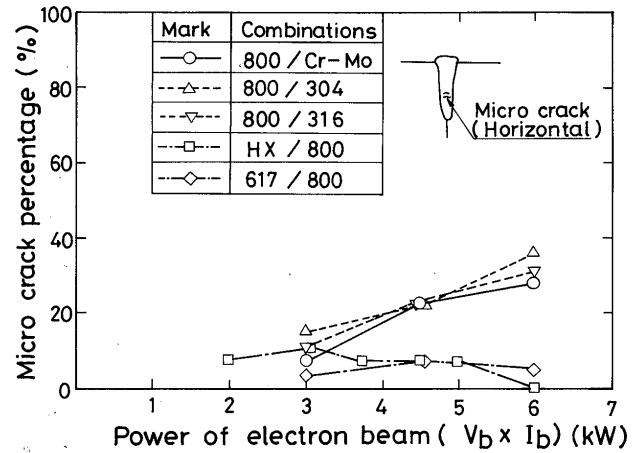


Fig. 10 Effect of electron beam power on micro crack percentage

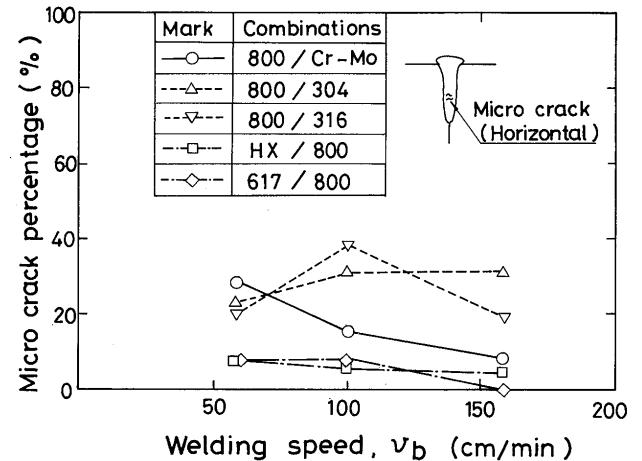


Fig. 11 Effect of welding speed on micro crack percentage

with Hastelloy X and Inconel 617 do not show any correlation. However the relatively large horizontal and vertical cracks (200  $\mu$ m or more) generated only for the welding conditions of maximum beam power of 6 KW ( $V_b = 150$  KV,  $I_b = 40$  mA) in this experiment.

Relation between horizontal crack percentage and welding speed is shown in Figure 11. As for the combination of Incoloy 800H and 2.25Cr-1Mo, crack percentage shows the tendency to decrease as the welding speed increases, and no correlation is observed for other combinations.

In summary, correlation between micro crack and welding conditions, which will generally be applied to all the combination of dissimilar materials, could not be observed. Though, as described in section 4.3, a sort of correlation can be found when micro crack generation zone is obtained for each combination of dissimilar materials changing  $a_b$  as a parameter, while fixing the other welding parameters.



### 4.3 Adequate Welding Conditions

It is found that such weld defects as described in section 4.2 will generate in dissimilar welded joints of superalloys welded by the electron beam welding. In order to obtain region of adequate welding condition where no weld defects generate for each dissimilar welded joint, defect generation area is illustrated in correlation diagram of  $a_b$  value and penetration depth for each welded joint.

As example of this area, area for combination of Incoloy 800H/2.25Cr-1Mo is shown in Figure 12, that for Incoloy 800H/SUS304 is shown in Figure 13, and that for Hastelloy X/Incoloy 800H is shown in Figure 14. Though weld defect (R-porosity and micro crack) generation areas are different from one combination to another combination of dissimilar materials, the followings are described in general.

R-porosity will generate in the specific zone of  $a_b$  value, provided that  $V_b \times I_b/v_b$  is constant, and will not generate for the value which is lower or higher than the specific value. Also it is clear that the smaller  $V_b \times I_b/v_b$ , the narrower the  $a_b$  value zone where R-porosity will generate. On the contrary, micro crack (horizontal and vertical crack) will generate lower than the specific  $a_b$  value or higher than the value, provided that  $V_b \times I_b/v_b$  is constant, and will not generate between this specific value. This specific value  $a_b$ , which decides the generation of micro crack, differs for the value of  $V_b \times I_b/v_b$ , but there is no particular correlation between  $a_b$  value and  $V_b \times I_b/v_b$ . Accordingly, the region of adequate welding condition, where neither R-porosity nor micro crack will generate, becomes pretty narrow. Though, it is clear from Fig. 12 to Fig. 14 that the region of adequate welding condition, which covers the thickness of 15 mm, will exist

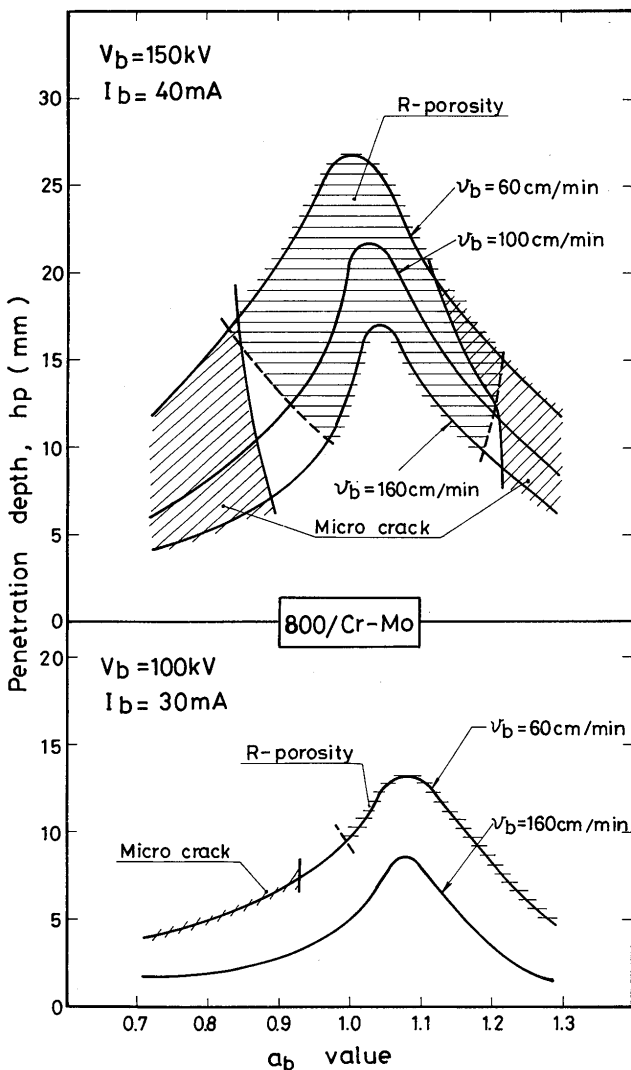


Fig. 12 Effect of  $a_b$  value and penetration depth on weld defects (Incoloy 800H/2.25Cr-1Mo steel)

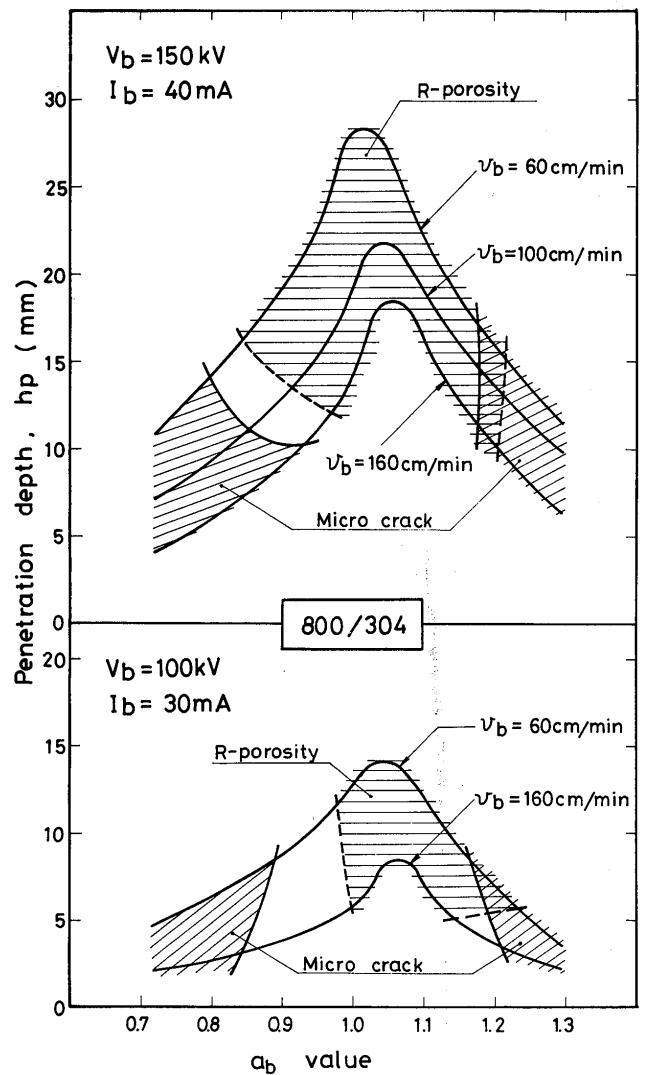


Fig. 13 Effect of  $a_b$  value and penetration depth on weld defects (Incoloy 800H/SUS304)

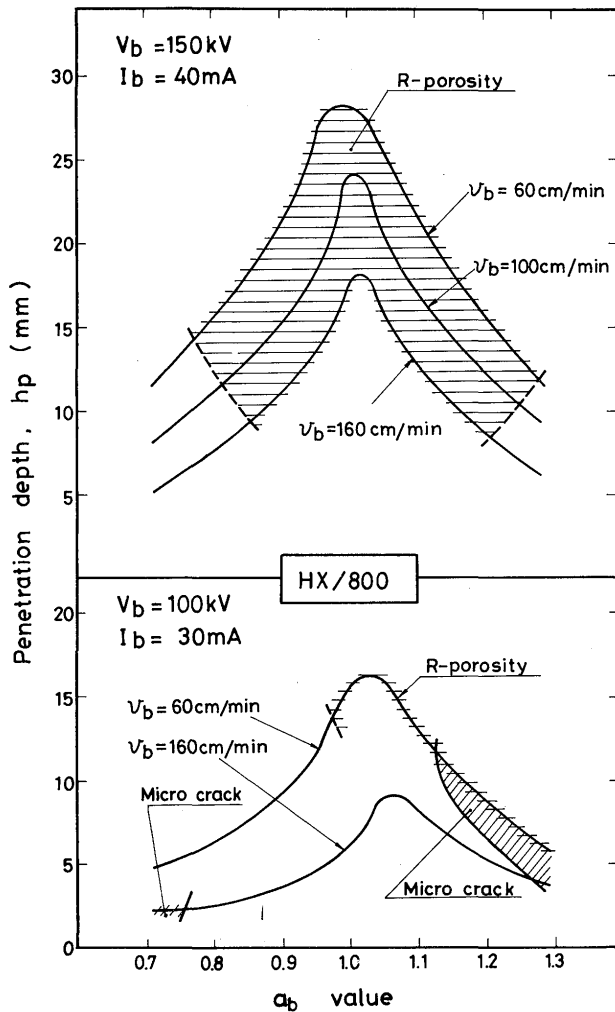


Fig. 14 Effect of  $a_b$  value and penetration depth on weld defects (Hastelloy X/Incoloy 800H)

for either combination of dissimilar materials under the condition of this experiment.

In applying the electron beam welding to manufacturing the products, underlip structure is used, and the underlip is usually removed at final stage, resulting the removal of R-porosity. As a result, the region of adequate welding condition becomes fairly wide.

Other combinations of dissimilar materials except the combination with Inconel 617 has similar tendency as above, and can cover the thickness less than about 15 mm. As for combination with Inconel 617, nail-head crack generates on bond of Inconel 617 side without respect to  $a_b$  value, and can not get non-defect welding condition.

## 5. Conclusion

In this paper, for various welded joints of dissimilar materials for nuclear plant welded by the electron beam welding, the effect of welding conditions on the gener-

ation of weld defects is studied, and the region of adequate welding condition is obtained for each combination of dissimilar materials. The result obtained are as follows.

- (1) For every combination of dissimilar materials in this experiment, the almost symmetrical weld bead is obtained by locating the center of electron beam on the center of square butt welded joint. Under the same welding condition, nearly same penetration depth and bead configuration are obtained for either combination.
- (2) Defects generated at weld zone are R-porosity and micro crack, and the latter is composed of nail-head crack, which generates at nail head, and solidification crack (horizontal and vertical crack), which generates along the dendrite boundary of weld metal.
- (3) R-porosity occurs in all the combination with no relation to the materials, and it generates within the specific range of  $a_b$  value. It does not generate lower than that value nor higher than that value. As the smaller the value of  $V_b \times I_b / v_b$ , the range of  $a_b$  value, within which R-porosity will generate, becomes narrower.
- (4) Most of nail-head crack occurs in the combination with Inconel 617, and runs almost normal to bond at nail head of Inconel 617 side, existing between weld metal and heat affected zone. The nail-head crack occurs at any welding condition, almost without respect to welding condition.
- (5) The solidification crack (horizontal and vertical crack) is observed mostly in the combination with Incoloy 800H, and is seldom observed in that with Inconel 625. In contrast to the generation area of R-porosity, this crack generates at lower or higher than the specific  $a_b$  value, and does not occur between these values. No specific effect of  $V_b \times I_b / v_b$  on the occurrence of this crack is observed.
- (6) For each combination of dissimilar material, defect generation area is illustrated in the correlation diagram between penetration depth and  $a_b$  value to obtain region of adequate welding condition. As results, the region of adequate welding condition, which covers the thickness less than about 15 mm, is found to exist except for the combination with Inconel 617, though the region of non-defect is narrow. In welding the product, the underlip structure is used, and this underlip is usually removed at the final stage. And so R-porosity becomes no problem, and the region of adequate welding condition becomes fairly wide. On the other hand, the nail-head crack runs the wide area and non-defect area can not be observed for the combination with Inconel 617.

## References

- 1) Y. Arata: "Terms and Definitions Proposed from Japan" IIW (1972).
- 2) Y. Arata, K. Terai et al.: "Fundamental Studies on Electron Beam Welding of Heat-resistant Superalloys for Nuclear Plants (Report 1)", JWRI, Vol. 5, No. 2, 119-126 (1976).
- 3) Susei, Kutsuna, Yamamoto: "Study on Ni-base superalloy welding (Report 1)" Preprint of the National Meeting of the JWS, No. 25, 240-241 (1978) (in Japanese).
- 4) Y. Arata, K. Terai et al.: "Fundamentale Studien Zum Elektronenstrahl Schweißen von Hitzebeständigen Legierungen für Kernkraftanlagen (Bericht 3)", JWRI, Vol. 6, No. 2, 75-90 (1977).